5th International Symposium on Three-Dimensional Electromagnetics
Sapporo, Japan, May 7-9, 2013

Frequency-domain 3D geo-electromagnetic modeling with sub-domain Chebyshev spectral method

Bing Zhou, Graham Heinson and Aixa Rivera-Rios
Department of Geology and geophysics, The University of Adelaide

SUMMARY

We propose a new numerical modeling method for 3D geo-electromagnetic fields which are measured in magnetotelluric or controlled-source electromagnetic survey. The new scheme utilizes a curved coordinate system to match the free-surface topography and subsurface interfaces, and applies the Chebyshev spectral method to differentiations of the generalized governing equations. We adapt the normal global differentiation scheme to a sub-domain scheme so that the assembled matrix becomes sparse but remains having high accuracies for the numerical differentiations. Our numerical tests show that the sub-domain Chebyshev differentiations are superior to the traditional finite-difference methods in the accuracy of differentiations. Meanwhile, we investigated the effectiveness of the generalized perfectly matched layer applied to the 3D modeling. The initial results show success in removing the influences of artificial boundaries truncating the infinite computational domain into a reasonable size, and encourage us to explore more benefits of the proposed technique.

Keywords: geo-electromagnetic fields, 3D modeling, perfectly matched layer, Chebyshev spectral method.

INTRODUCTION

Geo-electromagnetic surveys, e.g. magnetotelluric (MT) and controlled-source electromagnetic (CSEM) measurements are often applied for mineral explorations, groundwater and geothermal investigations, and for imaging deep structures of the earth. To understand or interpret these data, many numerical methods, such as finite-difference (Aruliah et al. 2001; Wang and Fang 2001), finite-element (Jin at al.2007; Mukherjee and Everett 2011), integral equation (Zhdanov et al.2006), boundary element (Ren at al. 2012a) and some hybrid methods (Xie et al. 2000; Ren et al. 2012b) have been developed for 3D geo-electromagnetic modeling. Each of the numerical methods has its own advantages and disadvantages, or limitations to different geological models.

Here, we propose a new 3D modeling approach, called "sub-domain Chebyshev spectral method", which seeks a "strong" solution of the generalized governing equations of electromagnetic fields. This method can be applied to arbitrary anisotropic geological models, which may be given by the model parameter tensors of electric permittivity, magnetic permeability and conductivity, as well as having free-surface topography and subsurface interfaces. Main advantages of the proposed method are the high accuracy in numerical differentiations with a sparse assembled matrix and the capability to handle complex geological models.

In addition, we investigated the effectiveness of the generalized perfectly matched layer (GPML) applied to the governing equations. The preliminary results show success in removing the effects of artificial boundaries reducing the size of the computational domain, and inspired us to adopt this technique for 3D geo-electromagnetic modeling.

GOVERNING EQUATIONS

For general applications, we consider the following frequency-domain governing equation for 3D geo-electromagnetic fields:

$$\nabla\times(\mathbf{v}/i\omega\cdot\nabla\times\mathbf{F})+\boldsymbol{\kappa}\cdot\mathbf{F}=\mathbf{s}^{(F)}, \qquad (1)$$

where $\mathbf{F}\in\{\mathbf{E},\mathbf{H}\}$ may be the electric ($\mathbf{E}$) and magnetic ($\mathbf{H}$) field intensity responding to the model parameter tensors $\mathbf{v}\in\{\boldsymbol{\mu}^{-1},\tilde{\boldsymbol{\sigma}}^{-1}\}$ and $\boldsymbol{\kappa}\in\{\tilde{\boldsymbol{\sigma}},\boldsymbol{\mu}\}$; or it may be the secondary fields $\mathbf{F}\in\{\mathbf{E}^s,\mathbf{H}^s\}$ due to model changes $\{\delta\boldsymbol{\mu},\delta\tilde{\boldsymbol{\sigma}}\}$ from a reference model $\{\boldsymbol{\mu}_p,\tilde{\boldsymbol{\sigma}}_p\}$ and to the incidence of primary fields $\{\mathbf{E}^p,\mathbf{H}^p\}$. The model parameter tensors $\boldsymbol{\mu}$ and $\tilde{\boldsymbol{\sigma}}=\boldsymbol{\sigma}+i\omega\boldsymbol{\varepsilon}$ are the magnetic permeability and complex-valued conductivity, whose real part is the real conductivity $\boldsymbol{\sigma}$ and imaginary part is related to the electric permittivity $\boldsymbol{\varepsilon}$ of a geological model. The vector $\mathbf{s}^{(F)}$ is the source generating the field vector $\mathbf{F}$:

$$\mathbf{s}^{(F)}=\begin{cases}-\mathbf{j}_e, & (\mathbf{F}=\mathbf{E}),\\ \nabla\times(\tilde{\boldsymbol{\sigma}}^{-1}\mathbf{j}_e)/i\omega, & (\mathbf{F}=\mathbf{H}),\\ -[\delta\tilde{\boldsymbol{\sigma}}\cdot\mathbf{E}^p+\nabla\times(\boldsymbol{\mu}^{-1}\delta\boldsymbol{\mu}\cdot\mathbf{H}^p)], & (\mathbf{F}=\mathbf{E}^s),\\ -\delta\boldsymbol{\mu}\cdot\mathbf{H}^p+\nabla\times(\tilde{\boldsymbol{\sigma}}^{-1}\delta\tilde{\boldsymbol{\sigma}}\cdot\mathbf{E}^p), & (\mathbf{F}=\mathbf{H}^s).\end{cases} \qquad (2)$$

Here ω and $\mathbf{j}_e$ are the angular frequency and the (natural or artificial) external current density, respectively.

PERFECTLY MATCHED LAYER

Due to limitation of computer memory, it is common to employ some artificial boundaries truncating the "infinite" earth domain. At the artificial boundaries, most of researchers applied "known" values, i.e. 1D or 2D calculations (Mackie et al. 1993; Siripunvaraporn et al. 2002), or explicit expressions of the boundary values obtained by integral equations (Xie et al. 2000) or finite-boundary element approaches (Ren et al. 2012). The computations of boundary values are complicated and make the assembled matrix more computer consumptions.

Alternatively, considering that the electromagnetic fields are propagating or evanescent wave-fields, one may apply the so-called perfectly matched layer (PML) that absorbs the energies of electromagnetic fields in the artificial boundary zones and removes the effects of the artificial boundaries (Berenger 1994). Particularly, the mathematical implementation of the PML in the frequency-domain is much simpler than any other treatment of the artificial boundaries, so it becomes popular for frequency-domain electromagnetic and seismic wave-field modeling (Fang and Wu 1996; Zhou and Greenhalgh 2011). It is mathematically achieved by simply introducing stretching coordinate factors to the governing equations. Therefore, the computation of the global earth domain becomes that of a limited one without any influence of artificial boundaries to the solution in the central domain.

Here, we apply the generalized perfectly matched layer (GPML) presented by Fang and Wu (1996) and Cummer (2003) to eq.(1) and (2). It is done by applying the following partial differentiations of the stretching coordinates:

$$\partial_{\tilde{x}_j} = (1/h^{(x_j)})\partial_{x_j}, \quad h^{(x_j)} = 1 - ib(x_j) \tag{3}$$

to the artificial boundary zone (absorber) having the normal parallel to the x_j-axis, and simply choosing $b(x_j)$ as follows:

$$b(x_j) = c_0(|\mathbf{r}(x_j) - \mathbf{r}_a| / |\mathbf{r}_b - \mathbf{r}_a|)^n. \tag{4}$$

Here, c_0 and n are constant and may be properly determined in terms of the length $|\mathbf{r}_a - \mathbf{r}_b|$ of the PML. The vectors $\mathbf{r}_a$ and $\mathbf{r}_b$ stand for the two-ending points of the PML. We call $h^{(x_j)}$ the stretching factors which are functions of the coordinates $\{x_j\}$. After applying the stretching coordinate factors to eq. (1), it becomes

$$\tilde{\nabla} \times (\mathbf{v} / i\omega \cdot \tilde{\nabla} \times \mathbf{F}) + \boldsymbol{\kappa} \cdot \mathbf{F} = \tilde{\mathbf{s}}^{(F)}, \tag{5}$$

where the tilde-hat means the involvement of stretching coordinates. Note that the general curl-curl operator has now the following form:

$$\tilde{\nabla} \times (\mathbf{v} \cdot \tilde{\nabla} \times \mathbf{F}) = \varepsilon_{\alpha\beta\gamma}\varepsilon_{ijk} / h^{(x_\beta)} \partial_{x_\beta} (\nu_{\gamma i} / h^{(x_j)} \partial_{x_j} F_k). \tag{6}$$

Setting up

$$h^{(x_1+x_2+x_3)} = h^{(x_1)}h^{(x_2)}h^{(x_3)} \tag{7}$$

and multiplying $h^{(x_1+x_2+x_3)}$ to eq. (6), we have

$$\begin{aligned}&\varepsilon_{\alpha\beta\gamma}\varepsilon_{ijk}\partial_{x_\beta}(\nu_{\gamma i} h^{(x_1+x_2+x_3-x_\beta-x_j)}\partial_{x_j}F_k) + \\ &i\omega h^{(x_1+x_2+x_3)}\boldsymbol{\kappa}\cdot\mathbf{F} = h^{(x_1+x_2+x_3)}\mathbf{s}^F.\end{aligned} \tag{8}$$

Defining the new model parameter tensors:

$$\begin{aligned}&\tilde{\mathbf{v}} = \{\tilde{\nu}_{\gamma i}^{(\beta,j)}\} = \{\nu_{\gamma i} h^{(x_1)}h^{(x_2)}h^{(x_3)} / h^{(x_\beta)}h^{(x_j)}\}, \\ &\tilde{\boldsymbol{\kappa}} = h^{(x_1)}h^{(x_2)}h^{(x_3)}\boldsymbol{\kappa}, \quad \tilde{\mathbf{s}}^F = h^{(x_1)}h^{(x_2)}h^{(x_3}\mathbf{s}^F,\end{aligned} \tag{9}$$

we have eq. (6) in the following version

$$\nabla \times (\tilde{\mathbf{v}} / i\omega \cdot \nabla \times \mathbf{F}) + \tilde{\boldsymbol{\kappa}} \cdot \mathbf{F} = \tilde{\mathbf{s}}^{(F)}. \tag{10}$$

which is the governing equation incorporated with the GPML. Apparently, eq. (10) has the same form as eq.(1) except for the model parameter tensors and the source term, which involve the stretching coordinate factors $\{h^{(x_1)}, h^{(x_2)}, h^{(x_3)}\}$. Accordingly, solving eq. (1) for the geo-electromagnetic fields in the global earth is now changed into solving eq. (10) for the limited dimensions of the earth surrounded by the artificial boundaries.

CHEBYSHEV SPECTRAL METHOD

In mathematics, the solution of eq. (10) is often called a "strong" solution compared with the "weak" solution given by the finite element approach. This means that all of the field quantities involved in eq. (10) must be differentiable, i.e. the model parameter tensor $\tilde{\mathbf{v}}$ requires first-order differentiation and the field vector $\mathbf{F}$ needs second-order differentiations. The "weak" solution excludes the differentiability of model parameter tensors and only first-order differentiations of the field $\mathbf{F}$ are computed. However, seeking the "strong" solution is simple, straightforward and easy to program. So, it is very popular in geophysical modeling. Here, we apply the so-called "sub-domain Chebyshev differentiation scheme", which is a modified version of the normal global Chebyshev spectral method (Trefethen 2000), to the computations of partial derivatives of the governing equation. We divide the computation domain into sub-domains and in each sub-domain, we approximate the differentiations by

$$\begin{aligned}&\partial_\alpha F \approx \overline{\mathbf{D}}_\alpha^{(i,j,k)}\overline{\mathbf{F}}^{(i,j,k)}, \\ &\partial_{\alpha\beta} F \approx \overline{\mathbf{D}}_{\alpha\beta}^{(i,j,k)}\overline{\mathbf{F}}, \quad (\alpha, \beta = x, y, z),\end{aligned} \tag{11}$$

where $\overline{\mathbf{F}}^{(i,j,k)} = (F_{1x}^{(i,j,k)}, F_{1y}^{(i,j,k)}, F_{1z}^{(i,j,k)}, ..., F_{nx}^{(i,j,k)}, F_{ny}^{(i,j,k)}, F_{nz}^{(i,j,k)})$ are the discrete values of the field vector $\mathbf{F}$ in the (i,j,k)-th sub-domain. The differential vectors $\overline{\mathbf{D}}_\alpha^{(i,j,k)}$ are given by

$$\begin{aligned}&\overline{\mathbf{D}}_x^{(i,j,k)} = (2/\Delta x_i)\mathbf{D}_\xi^{(i,j,k)} - (2/\Delta z_k(x,y))\partial_x z\mathbf{D}_\varsigma^{(i,j,k)}, \\ &\overline{\mathbf{D}}_y^{(i,j,k)} = (2/\Delta y_j)\mathbf{D}_\eta^{(i,j,k)} - (2/\Delta z_k(x,y))\partial_y z\mathbf{D}_\eta^{(i,j,k)}, \\ &\overline{\mathbf{D}}_z^{(i,j,k)} = (2/\Delta z_k(x,y))\mathbf{D}_\varsigma^{(i,j,k)}.\end{aligned} \tag{12}$$

Here $\{\Delta x_i, \Delta y_j, \Delta z_k(x,y)\}$ are the dimensions of the (i,j,k)-th sub-domain, $\{\partial_x z, \partial_y z\}$ are the tangents of the free-surface topography or subsurface interfaces approached by 2D cubic spline interpolations, and $\{\mathbf{D}_\xi, \mathbf{D}_\eta, \mathbf{D}_\varsigma\}$ are the Chebyshev differential vectors with the points in the sub-domain. At the sharing points or the boundary point between sub-domains, we employ the Lagrange differential vectors with the nearby Chebyshev points for $\{\mathbf{D}_\xi, \mathbf{D}_\eta, \mathbf{D}_\varsigma\}$.

Applying eq. (11) into (10) for every Chebyshev point in the domain and assembling all of the sub-domain differential vectors, we obtain the linear system of equations

$$\mathbf{A}\overline{\mathbf{F}} = \overline{\mathbf{b}}\,, \tag{13}$$

where $\mathbf{A}$ is a large, sparse matrix, $\overline{\mathbf{F}}$ and $\overline{\mathbf{b}}$ are the vectors whose components are the discrete values of the field $\mathbf{F}$ and the source vector $\tilde{\mathbf{s}}^{(F)}$.

To solve eq. (13), an iterative solver, e.g. Krylov methods (Henk 2003), or direct methods, like SuperLU (Li and Demmel 2003), PARDISO (Schemk and Gartner 2004) and MUMPS (grail.ens-lyon.fr/mumps) can be used. The iterative solver spends much less computer memory and is often applied to a few right-hand-side vectors. In contrast, the direct method requires huge memory but is suitable for a large number of the right-hand-side vectors, e.g. 3D geo-electromagnetic modeling for inversion. We prefer MUMPS, a newly-developed parallelized linear-system solver, which may improve the computational efficiency of 3D geo-electromagnetic modeling and inversion.

EXPERIMENTS

We designed a 3D model given in Fig.1, which has

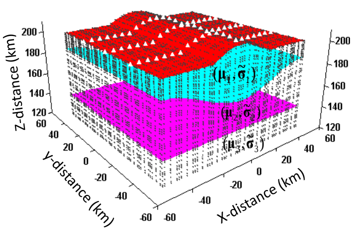

Figure 1. 3D geological mode for numerical experiments.

three layers and free-surface topography gridded by the sub-domain Chebyshev points (Trefethen 2000).

To examine the accuracies of numerical differentiations on the proposed method (eq. (11)), we distributed a known analytic function in the gridded model shown in Fig.1. Therefore, the exact derivatives are known and employed to calculate errors of the proposed method, as well as to compare with the traditional finite-difference (FD) approach based on the equal spaces in Fig.1. Fig.2 gives the maximum absolute relative errors of six derivatives, which show that the sub-domain Chebyshev differentiations (SCD) are superior to the traditional finite-difference and these results inspired us to apply eq. (11) to eq. (10).

To test the effectiveness of the GPML, we set up an isotropic model $(\boldsymbol{\mu}_1 = \boldsymbol{\mu}_2 = \boldsymbol{\mu}_3 = \mu_0\mathbf{I}$, $\tilde{\boldsymbol{\sigma}}_1 = (0.2 + i\omega\varepsilon_0)\mathbf{I}$, $\tilde{\boldsymbol{\sigma}}_2 = (0.01 + i\omega\varepsilon_0)\mathbf{I}$, $\tilde{\boldsymbol{\sigma}}_3 = (0.002 + i\omega\varepsilon_0)\mathbf{I})$ in Fig.1, and repeated solving eq. (13) for MT fields without and having stretching coordinate factors (GPML) respectively. Fig.3 and Fig.4 give the results, in which the left and right panels are the solutions of 0.1 Hz without and having the GPML. Here, the superscripts 0 and 1 indicaate the x- and y-polarization respectively. The results demonstrate that without the GPML (left panels), the solutions show asymmetric patterns caused by the artificial boundaries, but the results yielded by the GPML (right panels) are all symmetric and present no any artificial distortions. These results are reasonable because of the 2D isotropic geological structures in Fig.1.

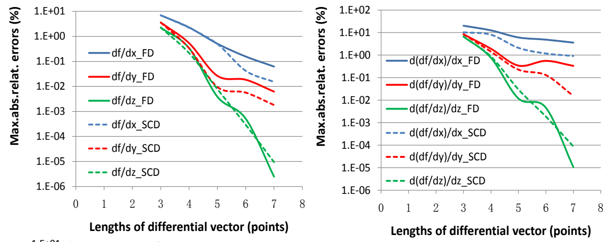

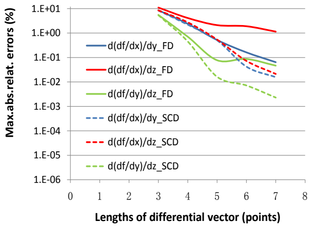

Figure 2 comparisons of sub-domain Chebyshev different-iations (SCD) with finite differ-ence (FD).

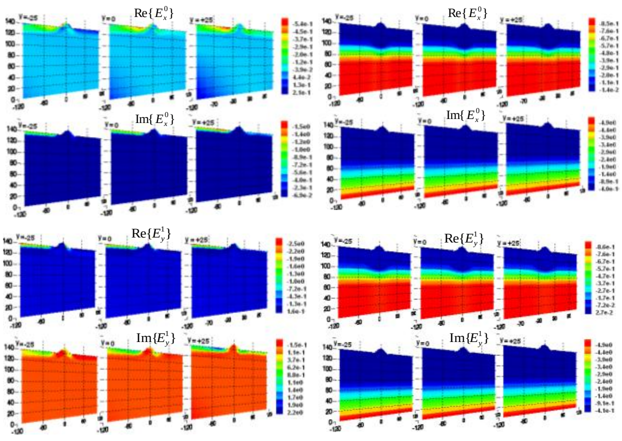

Figure 3 Solutions of the electric fields at 0.1 Hz without (left panel) and having (right panel) the GPML. The unit of distance is km.

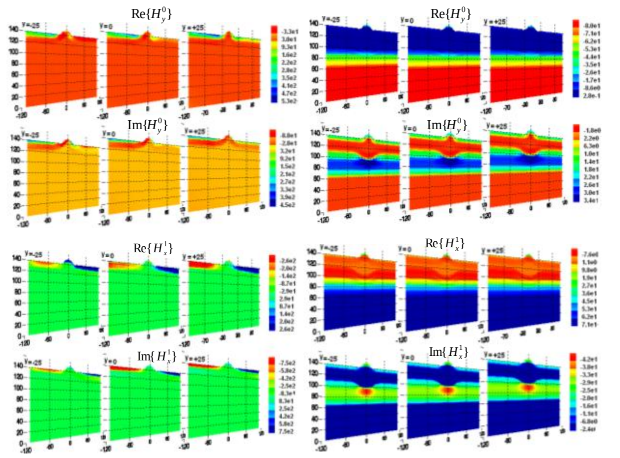

Figure 4 Solutions of magnetic fields at 0.1 Hz without and having the GPML. The unit of distance is km.

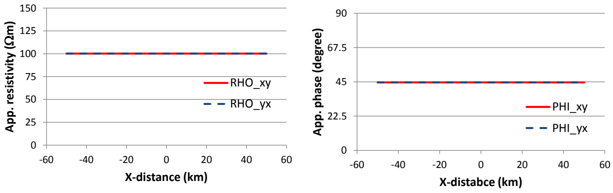

Figure 5. Modeling results of a homogeneous model ($\rho = 100\ \Omega$m, $\varepsilon = \varepsilon_0$, $\mu=\mu_0$, $f = 0.1$ Hz)

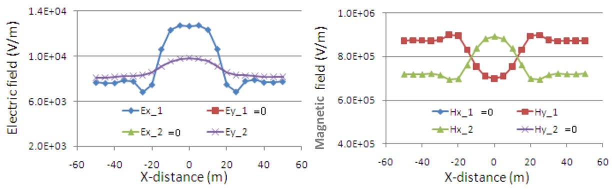

Figure 6 Modeling results of electromagnetic fields at 0.1 Hz along surface central profiling of the 3D geological model shown in Figure 1.

Fig.5 gives modeling results of a homogeneous model, from which one can see that the computed apparent resistivity and phase, are very close to true values of 100 Ωm and 45 degree. The errors are less than 2%. Fig.6 gives the central-profiling electromagnetic fields induced by two polarization directions in the model shown in Fig.1. These results show the variations of the fields due to a hill. We will continue such modeling experiments to explore the capability of the new approach to complex geological model.

CONCLUSIONS

A modified version of Chebyshev spectral method is presented for 3D geo-electromagnetic modeling. The main feature of the new method is the replacement of global differentiations in common Chebyshev spectral method by a sub-domain differential scheme, so that the assembled matrix becomes sparse. However, it remains having higher accuracies for spatial derivatives in the governing equations than traditional finite-difference method. It also has the capability to deal with complex geological model that may be isotropic or anisotropic rocks given by the parameter tensors of magnetic permeability and complex-valued conductivity.
Preliminary MT experiments show that the GPML remove the effects of artificial boundaries and truncate the "infinite" earth reducing the size of the computational domain. These results demonstrate that the implementation of sub-domain Chebyshev spectral method and incorporation of GPML are simple, general and applicable for 3D frequency-domain geo-electromagnetic modeling. However, further calibrations of this method are still required with more geological models.

ACKNOWLEDGEMENT

This work was supported by the Australian Research Council with a Discovery Project (DP)1093110).

REFERENCES

Aruliah, D. A., Ascher, U. M., Haber, E. and Oldenburg, D. (2001) A method for the forward modeling of 3-D electromagnetic quasi-static problems, Mathematical models and methods in applied sciences 11 1-21

Berenger, J. P., (1994), A perfectly matched layer for the absorption of electromagnetic waves, Journal of computational physics 114 186-200.

Fang, J., and Wu Z., 1996, Generalized perfectly matched layer for absorption of propagation and evanescent waves in lossless and lossy media, IEEE Transactions on Microwave theory and Techniques 44, No.12 2216-2222.

Henk, A. (2003) Itrative Krylov methods for large linear systems, Cambridge University Press, UK

Jin, M., Kim, H. J., Song, Y., Lee, T. J., Son, J. S. and Suh, H. (2007) 3D magnetotelluric modeling including surface topography, Geophysical Prospecting 55 277-287

Li, X. S. and Demmel, J. W. (2003) SuperLU_DIST: a scalable distributed-memory sparse direct solver for unsymmetric linear systems, ACM Truns. Math. Softw. 29 110-140

Mackie R. L., Madden T. R. and Wannamaker P. E. (1993) Three-dimensional magnetotelluric modeling using difference equations-theory and comparisons to integral equation solutions, Geophysics 58 215-226.

Mukherjee, S. and Everett, M. (2011) 3D controlled-source electromagnetic edge-based finite element modeling of conductive and permeable heterogeneities, Geophysics 76 p215-p226

Ren, Z., T. Kalscheuer, S. Greenhalgh, H. Maurer, 2012, Boundary element solutions for broadband 3D geo-electromagentic problems accelerated by multi-level fast mutlipole method, Geophys. J. Int. http://dx.doi.org/10.1093/gji/ggs043

Ren, Z., T. Kalscheuer, S. Greenhalgh, H. Maurer, 2012, A hybrid boundary element-finite element approach to modelling plane wave 3D electromagnetic induction responses in the Earth, Journal of Computational Physics, in press.

Schenk, O. and Gartner, K. (2004) Solving unsymmetric sparse system of linear equations with PARDISO, J. Future Gener. Comput. Syst. 20 475-487

Siripunvaraporn, W., Egbert G., and Lenbury Y. (2002) Numerical accuracy of magnetotelluric modeling: A comparison of finite difference approximations, Earth Planets Space, 54 721-725.

Trefethen L. (2000) Spectral methods in MATLAB, Oxford University Press, Oxford, England.

Wang, T. and Fang, S. (2001) 3-D electromagnetic anisotropy modeling using finite differences, Geophysics 66 1386-1398

Xie G., Li J., Majer E., Zuo D. and Oristaglio L. (2000) 3-D electromagnetic modeling and nonlinear inversion, Geophysics 65 804-822.

Zhdanov, M., Lee, S. K. and Yoshioka, K. (2006) Integral equation method for 3D modeling of electromagnetic fields in complex structures with inhomogeneous background conductivity, Geophysics 71 G333-G345.